THE ASTROPHYSICAL JOURNAL, 427:745–758, 1994 June 1

EVOLUTION OF SPIRAL GALAXIES. III. APPLICATION OF THE MULTIPHASE MODEL TO THE GALACTIC DISK

FEDERICO FERRINI,[1] MERCEDES MOLLÁ,[2] MARIA CHIARA PARDI,[3] AND ANGELES I. DÍAZ[2]
Received 1993 March 1; accepted 1993 December 2

ABSTRACT

We present an application of the multiphase model of Ferrini and coworkers, developed for the solar neighborhood, to other regions of the disk of the Galaxy in order to reproduce the observed element abundance gradients. The model describes the Galaxy as a two-zone system (halo and disk) sliced into nine cylindrical concentric regions and studies the time evolution of the five populations which inhabit the Milky Way: diffuse gas, molecular clouds, low-mass ($m < 4\ M_\odot$) and high-mass stars, and stellar remnants.

Our final aim is to reproduce the metallicity gradients that are observed in the Milky Way and in other external galaxies. We analyze the evolution of these gradients in time in order to relate their behavior to other galactic quantities such as the star formation rate and the infall rate.

The model describes the Galaxy by fitting a large number of observational constraints: abundance gradients, age-metallicity relations for disk and halo, both gas and mass distributions (including radial differences in the characteristic shapes of atomic and molecular gas), and radial distribution and history of star formation rate. The time evolution of abundance gradients is computed, revealing a flattening of gradients with time. In particular, the oxygen abundance was steeper at early times as a consequence of a larger infall. Since the disk is evolving and the gas is consumed, a saturation level is reached in every ring and the gradient will decrease to a minimum value.

Subject headings: galaxies: abundances — galaxies: evolution — galaxies: spiral

1. INTRODUCTION

Our Galaxy is a nonuniform system; indeed, various observations point out that a few quantities vary along the galactocentric radius, in particular, the gas and mass density and the element abundances. The radial distributions of these quantities are not the same, although they are connected through the star formation processes: the evolution of the Galaxy is, in short, the history of the transformation of diffuse gas into stars via the cloud phase, which in turn restores processed material to the gaseous placenta. The surface density of molecular gas has a plateau in a ring 3–8 kpc and decays with a scale length similar to that of the visible disk, decreasing by a factor of 2 from 6 to 15 kpc. The H I distribution has a surface density that is almost constant at radius up to the solar distance ($R_\odot$) and then increases by about a factor of 2.

Furthermore, element abundances show a radial gradient too. The first attempts to explain the abundance gradients, present in other spiral galaxies (see, e.g., Díaz 1989; Pagel 1989), were done in the framework of the simple model for galactic evolution (see, e.g., Tinsley 1980): within it, only a steep slope in the gas fraction could produce the observed abundance gradient. Its failure has been ascribed to various intrinsic oversimplifications, such as the instantaneous recycling approximation (IRA), the fact that it treats the Galaxy as a closed box, or the absence of radial flows. The crucial point is in fact a different one, residing only in the fundamental assumptions of the simple model and resulting in the independence of element abundances from star formation (SF) history (see Pardi & Ferrini 1994, hereafter Paper II). The hypothesis of a star formation rate (SFR) ψ proportional to the gas density (surface or volume, atomic, molecular, or total) together with the IRA leads to a relationship between chemical abundances and the SFR that is exceedingly simple considering the complex evolution of the Galaxy. Such a relationship also contradicts observations of radial distributions of gas density and SFRs, as we will show in the following.

We discuss briefly a few relevant papers in which authors tried to overcome the difficulties of the simple model by introducing several physical processes. In the Lacey & Fall (1983) model, metal-free gas falls into the disk at a rate exponentially decreasing with time [$f = f_0 \exp(-t/t_f)$]. Stars are formed within the standard Schmidt's scheme, with a rate proportional to a power of the volume gas density ($\psi \propto \rho^n$). The comparison with observations of radial distributions of gas fraction and SFR fixes the values of $t_f = 5.5$ Gyr if $n = 1$, or $t_f = 3.5$ Gyr if $n = 3/2$. In order to reproduce the observed abundance gradients, Lacey & Fall suggested that the timescale t_f should be a radial function, $t_f(r)$, increasing by a factor of 10 from 4 kpc to 14 kpc. Another possibility suggested by these authors is the existence of a critical gas density value such that SF will not take place for lower densities; in this case infall will last for a long time before stars form.

Since this seminal paper, a few models of chemical evolution have been developed to reproduce abundance gradients and gas fraction distributions. Most of them relax the IRA and use stellar mean lifetimes, with a variety of assumptions about the initial mass function (IMF), the SFR, and the infall rate laws. In essence we may classify the models into two main classes: (1) local models, which extend the solar neighborhood analysis to the Galactic disk, where every region evolves independently, and (2) radial flow models, which present exchange of mass in the disk via radial motions of gas (Lacey & Fall 1985;

[1] Dipartimento di Fisica, Sezione di Astronomia e Astrofisica, Università di Pisa, Piazza Torricelli 2, 56100 Pisa, Italia.
E-mail: federico@astrpi.difi.unipi.it.
[2] Departamento de Física Teórica, C-XI, Universidad Autónoma de Madrid, 28049 Madrid, Spain.
[3] Dipartimento di Fisica, Università di Milano, via Celoria 16, 20133 Milano, Italia.

Sommer-Larsen & Yoshii 1989; Clarke 1989). Local models found a gradient arising from different possibilities: (1) a variable yield depending on metallicity (Peimbert & Serrano 1982) or on a bimodal IMF (Güsten & Mezger 1983), (2) different dilution effects by infall (Díaz & Tosi 1984, 1986; Tosi & Díaz 1985), (3) a time scale of infall that varies with radius (Lacey & Fall 1985; Matteucci & François 1989), (4) radial dependence of SF law coefficients (Wyse & Silk 1989), (5) a gas density power index for the SFR law $n > 1$, and (6) the introduction of a critical threshold density value (Kennicutt 1989; Phillips & Edmunds 1991) or self-regulation in the SF processes (Parravano 1989, and references therein). There are also models with intermediate features (Tosi 1988; Götz & Köppen 1992) or related to hydrodynamical analyses (Burkert & Hensler 1988).

In general, all these models fit some of the observational constraints, but usually not all of them. Moreover, it has been shown that radial flows are not essential on obtaining gradients but that they may only amplify a gradient already present (Tosi 1988; Götz & Köppen 1992). Other simplifications are the use of the IRA, the noninclusion of Type I supernovae (hence the results for Fe are not meaningful), the infall of nonenriched or previously enriched material introduced without a correct treatment of the disk-halo connection, and finally the SF scheme.

This paper is an attempt to solve some of these difficulties through a proper and self-consistent treatment of several processes, in order to obtain an improvement in the understanding of gradients, not just to reproduce them. The paper is organized in the following way. In § 2 we present the physical model, while the observations for the quantities which vary with galactocentric radius are presented in § 3. Section 4 is devoted to a comparison of the present models results with observations. Section 5 deals with the conclusions about the physical processes relevant to determine the radial appearance of galactic disks.

2. THE EVOLUTION MODEL

We extend the multiphase and multizone model of Ferrini and coworkers to a large galactic region going from 4 to 12 kpc; the model has been described in Ferrini et al. (1992, hereafter Paper I). It is a two-zone model, in which the disk is a secondary structure formed by the gravitational accumulation from the halo. In each zone we allow for different phases of matter aggregation: diffuse gas (g), clouds (c) (except in the halo), and low-mass (s_1; $m < 4M_\odot$) and high-mass stars (s_2). The mass in the different phases changes through several conversion processes, defined and discussed in detail in Paper I, namely,

1. SF from gas-spontaneous fragmentation in the halo: $K_{1,2}\, g_H^n$
2. Cloud formation in the disk from diffuse gas: μg_D^n
3. SF from cloud collisions in the disk: $H_{1,2}\, c_D^2$
4. Diffuse gas restitution from cloud collisions in the disk: $H' c_D^2$
5. Induced SF via massive star-cloud interaction in the disk: $a_{1,2}\, c_D\, s_{2D}$
6. Diffuse gas restitution from induced SF in the disk: $a' c_D\, s_{2D}$
7. Formation of the disk through the accumulation of diffuse gas from the halo: $f g_H$

From the numerous observational and theoretical studies in the recent past, it is possible to describe the SF process on the basis of reasonable physical arguments (see, e.g., Franco 1991, 1992). SF is a two step process: first, clouds are formed from diffuse gas, then stars form from cloud collisions (spontaneous SF) or from the interaction of massive stars with clouds (stimulated SF); in the present simplified description devoted to a detailed study of the disk, stars form in the halo directly from diffuse gas by a sort of "Schmidt's law."

The IMF adopted here is the one computed following the nonlinear approach developed by Ferrini, Marchesoni, & Vulpiani (1983) and generalized by Ferrini, Palla, & Penco (1990) to take into account the simultaneous presence of various instability criteria in the definition of the critical mass for fragmentation. These authors consider an ensemble of clouds, representing a large volume of the interstellar medium, comparable to the size of a typical galactic giant molecular cloud complex. The ensemble presents a clumpy structure, with clouds distributed in mass and characterized by different physical conditions—namely, temperature, density, magnetic field strength, all properties determined thanks to the wealth of observational data available at present. The clouds experience a perturbation that triggers the onset of gravitational instability, and the physical processes controlling the critical mass for the instability may be of different natures (i.e., thermal, turbulent, magnetic). Finally, they compute the resulting IMF as being due to the superposition of the individual IMFs of the subunits of the ensemble. The weights of the components were chosen to yield a reasonable fit to the observed (local) IMF, and hence the IMF used in the present paper is equivalent to the observed local IMF. The statistical nature of the IMF so computed, the wide set of distributions for the cloud properties, and the theoretical analysis of the stochastic stability of the IMF (Ferrini 1991a) justify the assumption of an IMF constant in time and space.

Abundance evolution of 14 elements and their isotopes is computed: H, D, ^{3}He, ^{4}He, ^{12}C, ^{13}C, ^{16}O, ^{14}N, ^{20}Ne, ^{24}Mg, ^{28}Si, ^{32}S, ^{40}Ca, ^{56}Fe, and neutron-rich isotopes synthesized from ^{12}C, ^{13}C, ^{16}O, and ^{14}N. Starting from an initial composition of 24% ^{4}He (the rest hydrogen), the evolution of each element is followed using the formalism of *production matrices* $Q_{ij}(m)$, first introduced by Talbot & Arnett (1973), that give the fraction of the mass of an element j initially present in a star of mass m that is transformed into element i and ejected. A detailed description of the way these matrices are computed is given in Paper I. Here we briefly refer to the sources we used for the nucleosynthesis prescriptions.

Massive stars: 8 $M_\odot \le m \le 100$ $M_\odot$.—About the production of C, O, Ne, Mg, Si, S, Ca, and Fe, computations for several masses by Woosley & Weaver (1986, hereafter WW) concerning presupernova configurations have been considered. About explosive nucleosynthesis we refer again to Woosley and coworkers (Woosley, Pinto, & Weaver 1988). Prescriptions for the ^{14}N production are taken from Maeder (1983).

Low and intermediate mass stars: 0.8 $M_\odot \le m \le 8$ $M_\odot$.—Single stars and noninteracting binary systems contribute to the galactic chemical enrichment through winds or planetary nebula phases, releasing mainly He, C, and N; we follow the prescriptions of Renzini & Voli (1981).

Concerning the nucleosynthesis of Type Ia supernovae, we assume 0.6 $M_\odot$ of Fe and smaller quantities of C, O, Ne, Mg, Si, and Ca, according to the calculations of Nomoto, Thielemann, & Yokoi (1984); for Type Ib supernovae, we assume 0.3 $M_\odot$ in Fe and the remainder in He (Branch & Momoto 1986).

In recent years, there has been a serious effort by various authors to update stellar evolutionary models, both for quiet and for explosive phases of evolution. We mention in this regard the series for papers by Maeder and coworkers. Schaller et al. (1992) have evaluated the evolution of stars in the mass range 0.8–120 $M_\odot$ and for total metal contents (Z) 0.001 and 0.02 (solar). Schaerer et al. (1993) studied the same mass interval for $Z = 0.008$. The changes with respect to previous stellar models for the same group of stars concern the use of new opacities, accounting for moderate core overshooting, and the use of a new mass-loss rate. Comparing the yields resulting from these calculations with the yields produced by WW and Arnett (1991, hereafter A) has been done by Maeder (1992, hereafter M); in general, it is the case that for $Z = 0.001$ the yields by Maeder's group are not sensibly different from those of WW because the mass loss is not important. For $Z = 0.02$ and $M \geq 25\ M_\odot$, the produced and expelled masses of a few relevant elements are

$$M(^4\mathrm{He})_\mathrm{M}/M(^4\mathrm{He})_\mathrm{A} \simeq 1.3 \quad \text{for } M = 40\ M_\odot\ ,$$

$$\frac{M(^{12}\mathrm{C})_\mathrm{M}}{M(^{12}\mathrm{C})_\mathrm{WW}} \sim 4\text{–}5\ ,$$

$$\frac{M(^{16}\mathrm{O})_\mathrm{WW}}{M(^{16}\mathrm{O})_\mathrm{M}} \simeq 4\ ,$$

$$\frac{M(\mathrm{Z})_\mathrm{WW}}{M(\mathrm{Z})_\mathrm{M}} \simeq 4\ .$$

Differences grow when stellar mass increases: the wind is removing fuel from the structure. There are no dramatic differences from lower mass stars: the yields agree at various Z.

Differences in Ni production and in the production of very neutron-rich iron peak elements have been found by Nomoto and coworkers (Nomoto & Kondo 1991; Hashimoto, Iwamoto, & Nomoto 1993; Tsujimoto et al. 1993) in their new models for presupernova evolution and explosive nucleosynthesis.

It is reasonable to believe that the results for a few elements would be affected by the choice of the set of nucleosynthetic yields. In the absence of a complete set of reliable and coherent prescriptions for the element synthesis, we began a critical analysis of the present stellar nucleosynthesis calculations (Sandrelli 1994) and of their influence on galactic evolution. We abandoned the hypothesis of yields linearly correlated to initial abundances, especially for light elements and secondary elements, and we introduced new explosive nucleosynthesis yields (Timmes, Woosley, & Weaver 1993). We may conclude that, waiting for a new coherent set of calculations for low-mass and intermediate-mass stars at different metallicities with nonsolar element ratios and up to their latest stages of evolution, the present treatment of nucleosynthesis yields is not unreasonable.

Our aim is the application of the multiphase model to the Galactic disk in order to reproduce the abundance gradients and other constraints related to the radial distributions of mass, stars, gas, and so forth. Therefore, the model applied to the solar neighborhood in Papers I and II must be modified, not in the structure of the processes, but in the values of parameters which contain the typical timescales and efficiencies, because of the "microphysics" of the corresponding processes:

1. K-rate of gas conversion into stars in the halo. With a statistical argument, we can say that the SFR in the halo is directly proportional to the mass of diffuse gas and to the efficiency of the process (ϵ_K) and inversely proportional to the free-fall time necessary to accumulate mass by gravity and to form stars. From this we obtain

$$K(R) = \epsilon_K \sqrt{G/V_H(R)}\ , \tag{1}$$

where $V_H(R)$ is the volume of the halo as a function of the galactocentric radius R.

2. Cloud formation from diffuse gas is a similar process; therefore, the parameter μ amounts to

$$\mu(R) = \epsilon_\mu \sqrt{G/V_D(R)}\ , \tag{2}$$

where V_D is the volume of the disk at each radius. However, in this case the efficiency ϵ_μ may depend on radius because the spiral density waves are more strictly wound up in the inner regions than in the outer ones; hence, ϵ_μ will be larger at smaller radii.

3. SF by cloud collisions is represented by Hc^2; it is easily demonstrated that this term is proportional to the cloud number (n_c), to the cloud density (n_c/V_d), to the cloud mean mass ($\bar{M}_c$), to the cloud average cross section (A_c), to the mean free path for cloud collisions (λ), and to the inverse of the time needed to form stars during the cloud interactions (τ_*). Therefore, we may evaluate

$$Hc_D^2 = \frac{n_c^2}{V_D}\frac{\lambda}{\tau_*} A_c \epsilon_H \bar{M}_c\ ; \tag{3}$$

hence,

$$H(R) = \epsilon_H \frac{A_c}{V_D(R)}\frac{\lambda}{\tau_*}\frac{1}{\bar{M}_c}\ . \tag{4}$$

From the analysis of Ferrini et al. (1990) about cloud fragmentation, we obtain $\bar{M}_c = 3 \times 10^3\ M_\odot$. From Clifford & Elmegreen (1983), we obtain $A_c \sim 3 \times 10^3$ pc^2, and from Hausman & Roberts (1984), we estimate $\lambda \sim 200$ pc and $10^7 \leq \tau_* \leq 10^8$ yr. All these values are independent of galactocentric distance, with the exception of the volume of the disk.

4. a has been introduced to represent the coefficient of induced SF by the interactions of massive stars with molecular clouds. It may be considered to be independent of the distance: it is a local process, as discussed in Ferrini & Galli (1988), represented by the expression

$$a = \frac{1}{\langle \bar{m}_{s_2} \rangle} \epsilon_a (G\rho_c)^{1/2}\ , \tag{5}$$

where $\langle \bar{m}_{s_2} \rangle$ is the average mass of massive stars and ρ_c is the average cloud mass.

5. The most crucial parameter concerns disk formation from the halo: the infall rate parameter f. We assume it depends exponentially on galactic distance, following other authors (Lacey & Fall 1985; Götz & Köppen 1992):

$$f = f_0\, e^{-r/l}\ , \tag{6}$$

where l is a scale length that will be fixed properly by comparison with observations. The value of f_0 is related to the collapse timescale in the solar neighborhood (τ_{coll}) and will be considered as the only free parameter of the model, although in principle it can be fixed by the collapse conditions.

The Galaxy is modeled by nine cylindrical concentric regions 1 kpc wide extending above and below the Galactic

disk. Every region at the Galactocentric distance between 4 and 12 kpc has a different parameter set. The "best" parameters obtained in Paper II for the solar neighborhood have been used as "standard parameters," for the ring centered at the Sun position, $R = 8$ kpc. Our efficiencies ϵ are chosen in order to reproduce the standard parameters at the solar region. We varied the values around the standard ones to analyze their effect on radial disributions.

3. OBSERVATIONAL DATA

The detailed observations for the solar neighborhood have been reasonably well reproduced by the multiphase model (Paper II); here we present the set of observational constraints for the whole Galactic disk for which it is reasonable to require simultaneous fullfilment.

3.1. *The Interstellar Medium*

Many observational surveys exist regarding both the atomic and molecular components of the interstellar medium, which we correlate with our diffuse gas and cloud phases, respectively. The distributions are not always in agreement. In particular, the conservation factor from the CO emission to the H_2 density has been the subject of controversial work.

It is well established that the two phases have similar masses, but they are distributed in different ways: 85%–90% of molecular gas is within the solar radius, but only 30% of atomic gas is found in the same region. We chose to adopt as reference distributions the collection by Rana (1991), with the caveat that it reflects more a qualitative behavior than a truly quantitative constraint on the models. Indeed, there are data from other authors showing large differences from the ones we use; e.g., Sanders, Solomon, & Sloville (1984) found values a factor of 3 larger in their molecular distribution.

We corrected the values we considered, taking into account the radial variation of the conversion factor from CO to H_2 (χ) due to the different local conditions on molecular clouds. We adopted the results of Sodroski (1991) who determined the ratio for the outer Galaxy complexes. He derived the value 6.0×10^{20} molecules cm^{-2} K^{-1} s^{-1} as the best estimate for this ratio in the outer region, in agreement with Mead, Kutner, & Evans (1990) who investigated the variations between inner and outer zones of the Galaxy. In Table 1 we show that the radial distributions for the surface density of H I (col. [2]) and for molecular gas obtained with the value χ depending on radius (col. [3]) are different from the standard values for a constant χ (col. [4]). The modified ratio H_2/H I is in column (5).

TABLE 1

RADIAL GAS DISTRIBUTIONS

R (kpc) (1)	σ_{HI}[a] (2)	$\sigma_{H_2}[\chi(R)]$[a] (3)	$\sigma_{H_2}(\chi)$[a] (4)	H_2/H I (5)
4	2.61	3.77	9.20	1.44
5	2.56	4.44	8.72	1.73
6	2.94	4.20	6.89	1.43
7	3.09	2.69	3.32	0.87
8	3.25	2.05	2.05	0.63
9	4.80	1.59	1.30	0.33
10	6.19	1.13	0.73	0.18
11	5.99	3.51	1.81	0.50
12	5.35	1.83	0.75	0.34

[a] Densities in $M_\odot$ pc^{-2}.

Concerning the total mass distribution in the disk, we follow for the solar neighborhood the prescription by Gilmore, Wyse, & Kuijken (1989) which assigns to the solar neighborhood a mass density of $48 \pm 9\ M_\odot$ pc^{-2}. The radial mass distributions in the disk is assumed to be described by an exponential with a scale length of 3.5 kpc.

3.2. *Abundance Data*

The abundance data of oxygen we use for our Galaxy come from Shaver et al. (1983), obtained from H II region measurements, and from Faúndez-Abans & Maciel (1986) who observed type II planetary nebulae. In both cases a gradient exists, amounting to about 0.081 ± 0.017 dex kpc^{-1} for the first set and 0.091 ± 0.012 dex kpc^{-1} for the second set, after a scale change to normalize the solar Galactocentric distance to 8 kpc. A problem arises from the fact that abundance data come from a restricted region of the Galactic disk 2–3 kpc around the Sun. It is difficult to obtain reliable abundance determinations far away from the region. Fich & Silkey (1991) obtained from a sample of 18 H II regions only a few data for oxygen abundances, showing more a large dispersion than a clear trend.

When the electronic temperature is well measured, abundance data are calculated with a small error; however, there exists a great dispersion of data that only could be explained by inhomogeneities in the interstellar medium. This problem is related to an old and known one: the mean values for the solar neighborhood metallicities are similar to these values from other stars, but the O/H solar value is higher when compared with most H II regions at the solar Galactocentric distance. Hence, the model's results, predicting a correct O/H solar abundance, may produce a radial abundance distribution higher than the H II region's data.

Various possibilities have been suggested to solve this problem: first, depletion of oxygen into solid grains (Meyer 1988). This is supported by X-ray observations (Schattenburg & Canizares 1986) whose results for all oxygen atoms within the ISM amount to $12 + \log (O/H) = 8.87 \pm 0.12$, similar to the solar value. When the microturbulence is taken into account in a non–local thermodynamic equilibrium line-formation analysis, the differences between Shaver et al.'s data and abundance data derived from B stars can be justified (Fitzsimmons, Dufton, & Rolleston 1992). Therefore, we have also used this set of abundances as an observational constraint. A further solution to the problem would reside in a protosolar nebula enriched in ^{16}O by a supernova event; then the solar neighborhood would be an inhomogeneous region, but in this case the solar [Fe/H] value, similar to that of other stars of the same age, is rather hard to justify.

For nitrogen there are data from the same authors, but planetary nebulae are enriched in nitrogen due to dredge-up episodes in their progenitors; therefore, we used only Shaver et al.'s and Fich & Silkey's data. For sulfur, we may use Shaver et al.'s and Faúndez-Abans & Maciel's data; in both cases a more or less steep gradient exists.

We must stress that the quoted observations of Shaver et al. and Faúndez-Abans & Maciel refer to two different classes of objects. H II regions are young structures, deriving from recent episodes of SF, their presence being strictly connected to young massive stars, and their mean life being $\sim 10^6$ yr. In contrast, planetary nebulae of type II are members of an older population, corresponding to advanced evolutionary stages of intermediate-mass or loss-mass stars ($m < 7\ M_\odot$; see, e.g.,

Castellani, Chieffi, & Straniero 1990); these post–asymptotic giant branch stars may have a minimum age of 60×10^6 yr, but their age spread with a reasonable IMF can correspond to a population whose average age easily amounts to a few gigayears, considering that the typical mass of the objects involved may be around 2 $M_\odot$ ($\tau_{pn} \simeq 1.7$ Gyr; Castellani, Chieffi, & Straniero 1992). Hence, there is no doubt that these sets of observations reveal the radial abundance distributions of two different populations, which correspond to two distinct periods in the evolution of the Milky Way. It is then completely misleading to collect these data all together and consider them as a unique indication of a metallicity gradient. They are in fact evidence of gradients at two different times, and the fact that the slope for planetary nebulae is slightly steeper than for H II regions, if significant, can be an important constraint on the evolution models: it might tell us that the gradient was steeper at early times and then flattened at later times. The formation of the gradient would then be intrinsic to primitive disk formation and evolution, while the subsequent evolutionary phases would have contributed to the reduction of the abundance differences in the disk.

The variation of iron abundance with radial distance has been obtained for young clusters (Panagia & Tosi 1981; Cameron 1985), revealing a larger gradient for outer regions ($R > R_\odot$) than for inner regions, and for Cepheids (Harris 1981a, 1981b), where classical Cepheids (young stars) and type II Cepheids (old stars) correspond to two different times of galactic evolution. However, caution is needed when using these estimates because they are based on old isochrones, which have been questioned in recent years.

For old objects, we can use globular cluster data (Zinn 1985). These clusters are located at $0 \leq R \leq 6$ kpc and present a small gradient. We have only considered clusters at distances $4 \leq R \leq 6$ kpc to minimize any influence of the bulge component. Lewis & Freeman (1989) also measured the abundance for old K giant stars, but they found no evidence for a radial gradient.

It is obvious from these considerations that it is very important to obtain a homogeneous and large abundance data set for old and young objects, in order to determine the time behavior of the abundance gradients. The evolution of the Galaxy would be totally different, depending on whether these gradients increase of flatten with time.

3.3. *SFR*

The SFR as a function of the Galactocentric radius has been studied by Güsten & Mezger (1983), Lacey & Fall (1985), and Rana (1991). All these authors estimated the SFR from the H_α recombination line, which is directly related to the number of Lyman continuum photons emitted by massive stars.

Many quantities and hypotheses are involved in the determination of the SFR (see, e.g., Ferrini & Galli 1988). Nevertheless, these three independent anayses of the radial variation of the SFR give similar exponential distributions, except for the two most inner values in Güsten & Mezger's results, which appear to be depressed with respect to the others, perhaps due to the presence of a larger extinction. The present value of the SFR in the solar neighborhood is in the range 3.5–5 $M_\odot$ pc^{-2} Gyr^{-1}

3.4. *Age-Metallicity Relation*

We use three different age-metallicity relations (AMRs) for the solar neighborhood: the original AMR from Twarog (1980), the one from Carlberg et al. (1985) obtained with a revision of Twarog's data, and a new one from Barry (1988) measuring chromospheric ages of stars. Although the Carlberg et al. data show a larger dispersion, all three relations imply an almost constant value for the star metallicity in the last 7 Gyr and a rapid increase toward this value in the first 1–2 Gyr. Therefore, in this region a saturation level in the abundance is reached in a short time.

For the outer regions, far away the solar region ($R > 10$ kpc), we use the AMR from Geisler (1987), which presents a slow increase without reaching the saturation level at the present time. This behavior, as we will show in the following, can be due to the relative different rates of infall and SF.

3.5. *The* [O/Fe]-[Fe/H] *Relation*

Nissen & Edvardsson's (1992) data from F and G dwarfs provide a good set of abundances for the disk. According to these authors there is no universal [O/Fe]-[Fe/H] relation, but stars born in the inner parts of the early disk have higher [O/Fe] values at a given [Fe/H] than stars belonging to the outer disk.

4. RESULTS AND DISCUSSION

We present here the results of five models obtained by changing parameters as shown in Table 2: since the major role in shaping the gradients is played by f, the rate of accumulation from the halo, we focus the analysis on f, varying the assumptions both on the infall timescale at the solar radius τ_{coll} and on the radial exponential length scale l. We remind the reader that in principle $f(r, \tau_{coll})$ can be fixed by a proper treatment of the dynamical collapse of the Galaxy.

For simplicity, we keep fixed with respect to radius all the physical ingredients for the calculation of the other coefficients—i.e., efficiencies, cloud dimensions, velocity fields, and typical masses of massive stars—assuming that any radial change in the coefficients can only be due to volume (and therefore density) effects, with the exception of the efficiency of cloud formation, as stated in § 2. So the efficiency set of Table 2 is close to the values selected in Paper II for the disk evolution in the solar neighborhood.[4]

We start the review of results with model A defined by $\tau_{coll}(R_\odot) = 1$ Gyr and length scale $l = 2$. Figures 1 and 2, show plots of relevant quantities superimposed on the observational data discussed in the previous section: Figure 1*a* presents the SF histories (SF surface density normalized to the present surface density rate at the Sun ring, assuming $t_{now} = 13$ Gyr) for three-relevant radii (4, 8, and 12 kpc); Figure 1*b* shows the radial gradient of SFR at five different galactic ages; Figure 1*c* shows the iron temporal enrichment for the quoted radii;

[4] Before proceeding to analyze the results of the present model, we want to introduce a methodological note. We started this series aiming to provide an inquiry instrument to investigate the "jigsaw puzzle" (B. M. Tinsley) of galactic evolution. Two opposite, but complementary, attitudes could be taken: (1) to attack a single problem with specific tools or (2) to supply a scheme reflecting the intrinsic complexity of the problem. We follow the second road (Ferrini 1991b, 1993); this obviously does not mean that we will immediately introduce all the ingredients in the cauldron simultaneously or that we will supply a recipe for every problem, but rather we will cook slowly and add each ingredient in turn, tasting the flavor with each change. In our opinion, true predictions for external galaxies and close fits to the observational constraints in the Milky Way can only be produced after the introduction of bulge and the thick disk; so, in the following, we are not looking for a thorough correspondence of results with observations, but for indications of the relative importance of ingredients. This means, e.g., that radial changes would be invoked in the parameter space.

TABLE 2

PARAMETERS OF COMPUTED MODELS

Model	$\tau_{coll}(R_\odot)$ (10^7 yr)	Scale Length l (kpc)	Mass Distribution[a]
A.....	100	2	1
B.....	100	4	1
C.....	100	1	1
D.....	50	2	1
E.....	200	2	1
F.....	100	2	2
G.....	100	2	3

[a] Labels 1, 2, and 3 correspond, respectively, to solar ring masses 3, 4.5, and 1.5 × 10^9 $M_\odot$.

Figure 1*d* shows the radial gradient of total gas fraction (ratio of molecular and atomic gas to total mass in every ring) for the same ages as in Figure 1*b*. Figures 2*a*–2*e* plot, respectively, the oxygen, nitrogen, sulfur, carbon, and iron gradients at the five selected ages. Finally Figure 2*f* shows the relative behavior of iron and oxygen as [O/Fe] versus [Fe/H] in the three relevant rings.

1. Because the infall timescale is shorter at smaller radii, while the SF coefficients remain nearly constant (within a factor 2), the SF in the inner rings begins sooner and reaches higher values than in outer rings. Therefore, we can say that, whatever the model, inner SF histories are similar to a burst, while outer ones proceed at a nearly constant rate as shown in Figure 1*a*. The temporal behavior of the SFR radial gradient (Fig. 1*b*) is governed by the lowering of the total ring mass relative to the rise of τ_{coll} with radius. While at the beginning, the high gas supply at inner radii (due to both a higher M_{ring} and a quicker τ_{coll}) allows a very high SFR, as the gas in the center is exhausted (Fig. 1*d*) by infall termination and mass locking-up, the SFR radial distribution shows the behavior of Figure 1*b* for t = 13 Gyr. In fact, at outer radii both the continuing gas supply from the halo and the lower past SF efficiency produce a relatively high SFR. The temporal variation of gas amount at each radius compared to the radial change in evolu-

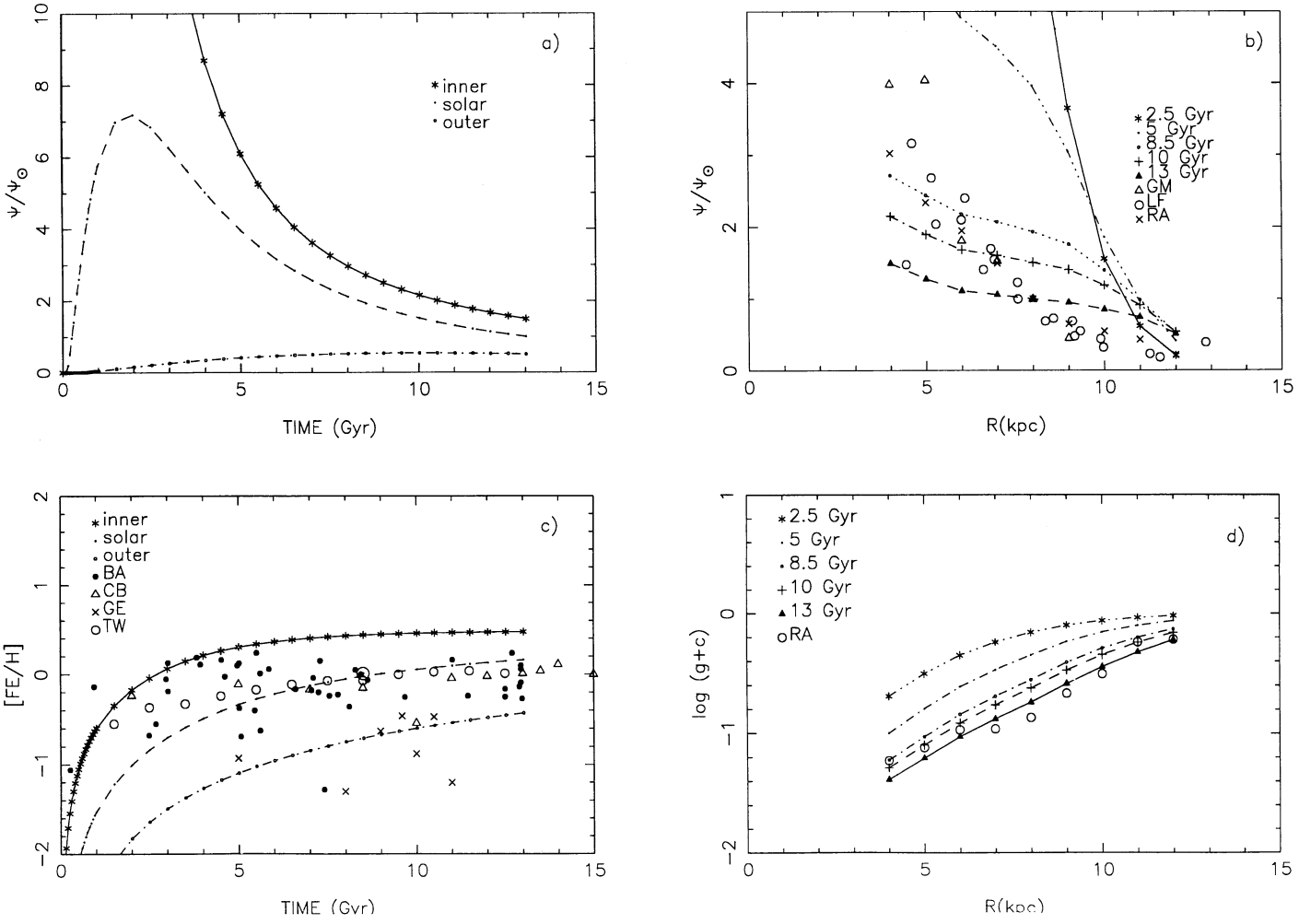

FIG. 1.—Model A. (*a*) SFR as a function of time for the three radii 4, 8, and 12 kpc, indicative of inner, solar, and outer regions; (*b*) SFR normalized to the solar neighborhood, at five different times; (*c*) AMR, i.e., the Fe enrichment history, for the three radii; GE data refer to outer regions; (*d*) Radial distribution of total gas fraction at five different times.

Key to abbreviations follows: BA: Barry 1988. CA: Cameron 1985. CB: Carlberg et al. 1985. FAM: Faúndez-Abans & Maciel 1986. FS: Fich & Silkey 1991. FZ: Fitzsimmons et al. 1992. GE: Geisler 1987. GM: Güsten & Mezger 1983. HA: Harris 1981a, yound Cepheids. HAO: Harris 1981b, old Cepheids. LF: Lacey & Fall 1985. NS: Nissen & Edvardsson 1992. PT: Panagia & Tosi 1981. RA: Rana 1991. SA: Sanders et al. 1984. SC: Schuster & Nissen 1989. SH: Shaver et al. 1983. TW: Twarog 1980. ZN: Zinn 1985.

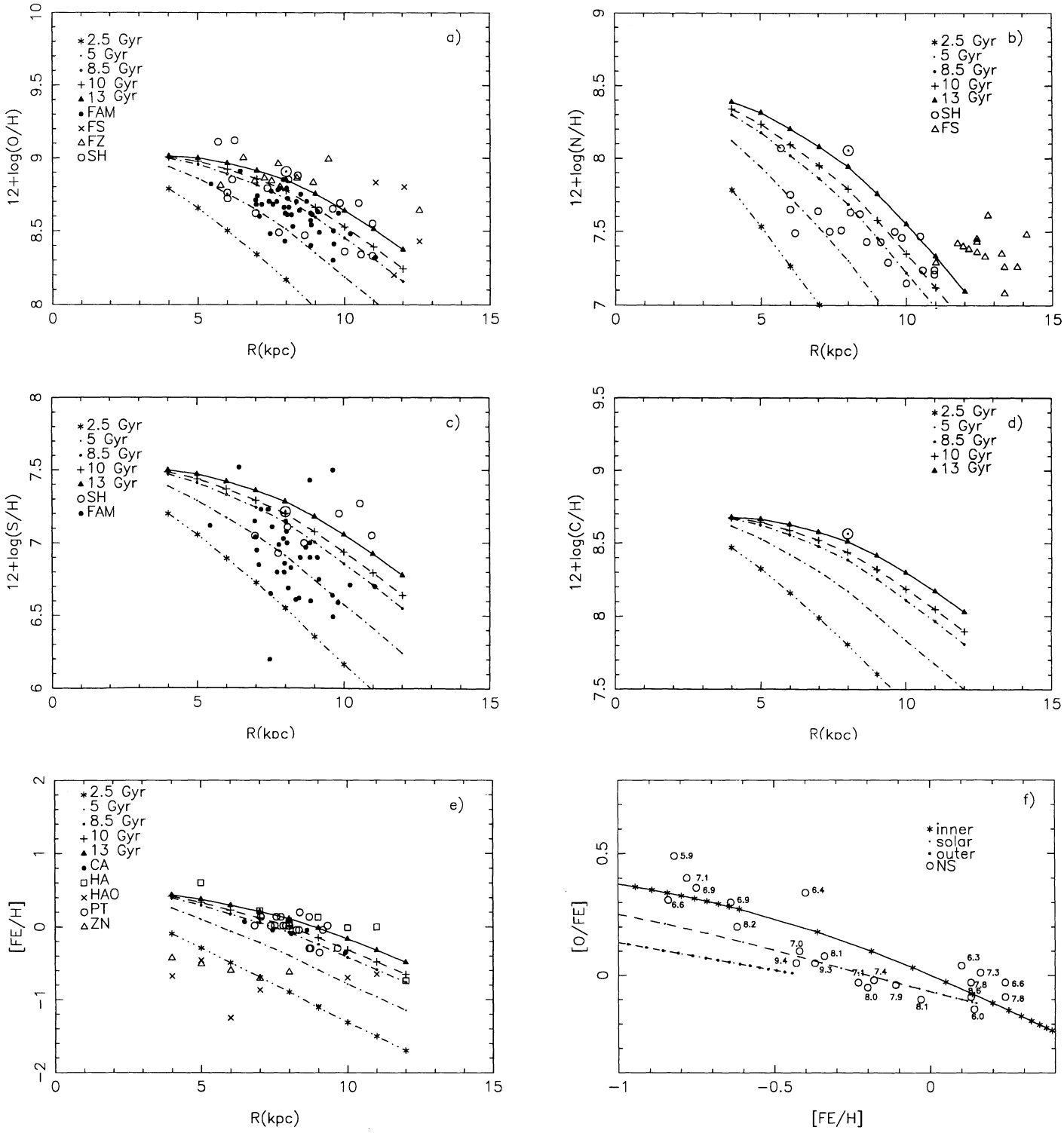

FIG. 2.—(*a*) Oxygen, (*b*) nitrogen, (*c*) Sulfur, (*d*) carbon, and (*e*) iron gradients at five selected times. ⊙ refers to solar values. (*f*) [O/Fe] vs. [Fe/H] at three radii of Fig. 1*a*. Numbers at every point are the object galactocentric distance from the NE data. See Fig. 1 caption for key to abbreviations.

tion coefficients can lead to the predicted double-peaked SFR gradients at late times. This model predicts a present SFR in the inner Galaxy that is lower than observed.

2. Both the enrichment histories (Fig. 1*c*) and the gas fraction gradients (Fig. 1*d*) can be understood in the framework of the above discussed SFR behaviors: as shown in Paper II, burstlike histories lead to a quicker rise in the abundance level, soon reaching the asymptotic value dependent on the total number of stars formed in the mass interval relevant to that particular element, while slow enrichments are linked to smoother SF histories. These arguments explain the predictions shown in Figure 1*c* of a steeper rise at inner radii than in

the outer Galaxy, in agreement with the observation of Geisler (1987).

3. For the gas fraction gradient, the predictions in Figure 1*d* show the progressive steepening expected on the basis of a quicker exhaustion in the interior. The prediction relative to the present (13 Gyr) radial distribution fits the observations perfectly.

The molecular cloud component decreases exponentially with radius (Fig. 3*a*), while the diffuse gas density is almost constant and rises in the outer regions, in agreement with observations. From the observed distributions, we may infer that a higher efficiency for the conversion of diffuse gas into molecular clouds and a lower one for cloud destruction are required at inner radii, while the opposite is the case at large radii, as assumed in the model, through the prescriptions for the parameters.

4. The relation between gas quantities and SFR (Fig. 3*b*) shows three different slopes for every radius, in a close similarity to Kennicutt's (1989) results (see his Fig. 8). Therefore the relation between gas density and SFR density is not a simple

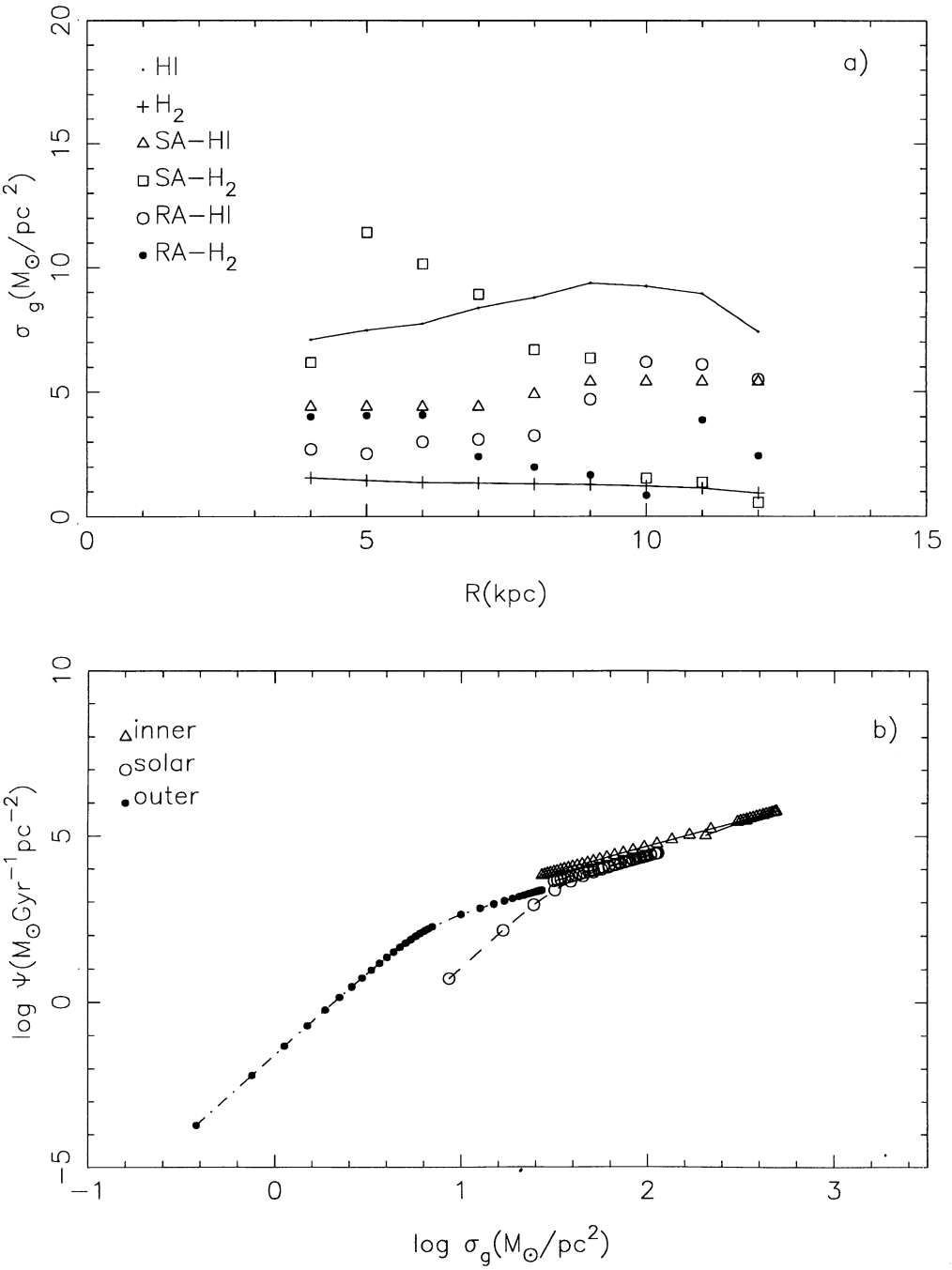

FIG. 3.—(*a*) Radial distribution of diffuse gas and cloud density. (*b*) Relation between gas density and SFR density for three radii of Fig. 1*a*. See Fig. 1 caption for key to abbreviations.

TABLE 3

OBSERVED AND COMPUTED GRADIENTS

	Young Objects			Old Objects		
Element Gradient (1)	Computed[a] (2)	Observed (3)	Reference to Column (3) (4)	Computed[b] (5)	Observed (6)	Reference for Column (6) (7)
d[O/H]/dR	−0.078[c]	−0.081	SH	−0.105	−0.091	FAM
		−0.167	FS			
		−0.027	FZ			
d[N/H]/dR	−0.160	−0.121	SH	−0.195	−0.093	FAM
		−0.073	FS			
d[C/H]/dR	−0.080			−0.107	−0.093	FAM
s[S/H]/dR	−0.089	0.043	SH	−0.114	−0.085	FAM
d[Fe/H]/dR	−0.113	−0.119	PT	−0.144	−0.06 (all)	ZN
					−0.100 ($R \leq R_\odot$)	
		−0.113	CA		−0.005 (all)	HAO
		−0.146	HA		−0.136 ($R \leq R_\odot$)	
					−0.182 ($R > R_\odot$)	

[a] Model at 13 Gyr.
[b] Model at 8.5 Gyr.
[c] Units are dex kpc^{-1}.

REFERENCES.—Key to abbreviations follows: CA: Cameron 1985. FAM: Faúndez-Abans & Maciel 1986. FS: Fich & Silkey 1991. FZ: Fitzsimmons et al. 1992. HA: Harris 1981a, young Cepheids. HAO: Harris 1981b, old Cepheids. PT: Panagia & Tosi 1981. SH: Shaver et al. 1983. ZN: Zinn 1985.

power law with an independent index, but a relation that changes and evolves with time, depending on the different gas phases present in each galactic ring.

5. The chemical gradients are soon established by ongoing SF, but as expected they flatten in time due to the progressive enrichment toward the asymptotic values at outer radii. Notwithstanding the large dispersion in the abundance gradient data for different elements, the distributions predicted in model A reproduce the observations quite well. These gradients can be obtained with other models; i.e., if ϵ_μ decreases by a factor 3, a good oxygen gradient is obtained, but in this case it is impossible to obtain the AMR with the same time of collapse, and with a more rapid collapse the gradient disappears. The computed gradients for oxygen, nitrogen, sulfur, carbon, and iron at two different times (13 and 8.5 Gyr) are shown in Table 3 compared with the observed ones for young and old objects.

6. The gradient for iron is shown in Figure 2*e*. In this case, the data represent metallicity estimates for stars or clusters in most cases. There are data for old objects (globular clusters from Zinn 1985 and type II Cepheids stars from Harris 1981a) and for young objects (young clusters from Panagia & Tosi 1981 and Cameron 1985 and classical Cepheids from Harris 1981b). Therefore, we can compare early and present gradients with the computed ones. For $R < R_\odot$, where the computed gradient flattens with time, the old object gradients (*crosses* and *triangles*) are slightly steeper than the ones from young clusters and stars (*squares*, *dots*, and *circles*).

A previous model (Mollá Díaz, & Tosi 1991) based on the "standard" scheme—the two free parameters (SFR and gas infall) included as analytic functions without a precise physical meaning—found that the gradient develops in the last 2 Gyr as a consequence of dilution due to infall on the galactic disk material; the gradient steepens with time, and the AMR in the last 5 Gyr is increasing for the inner part, flat for the solar region, and decreasing for the outer Galaxy; this last point contradicts observations. In our present model, the halo-disk coupling is responsible for the accretion of mass by the disk and, hence, for the SF. As the infall ceases, the SFR decreases and the abundances reach the saturation level. Since this occurs faster in the inner radius than in the outer regions, the abundance gradients become flatter with time (see Table 4; Mollá et al. 1992). As a consequence, early-type galaxies must have a flatter gradient, due to a higher degree of evolution, as seems to be observed in external galaxies (Oey & Kennicutt 1993).

7. Figure 2*f* presents the relation between iron and oxygen enrichment, which reflects the different origin of these two elements. At each radius, we find the expected oxygen overabundance due to delayed iron restitution from Type I supernovae. However, both the iron enrichment level at which this restitution begins and the oxygen overabundance level depend slightly on the radius, in accordance with the observations of Nissen & Edvardsson (1992): lower overabundance levels are to be expected in regions where the oxygen enrichment is slower and, therefore, Type I supernovae contribution (whose delay with respect to Type II supernovae is fixed only

TABLE 4

TIME EVOLUTION OF COMPUTED GRADIENTS

Time (Gyr)	d[O/H]/dR	d[N/H]/dR	d[C/H]/dR	d[S/H]/dR	d[Fe/H]/dR
2.5	−0.170[a]	−0.257	−0.181	−0.177	−0.201
5.0	−0.136	−0.229	−0.141	−0.144	−0.177
8.5	−0.105	−0.195	−0.107	−0.114	−0.144
10	−0.095	−0.182	−0.097	−0.104	−0.133
13	−0.078	−0.160	−0.080	−0.089	−0.113

[a] Units are dex kpc^{-1}

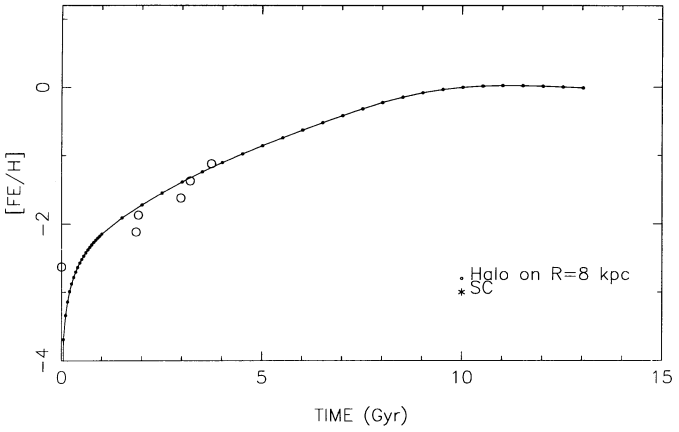

FIG. 4.—AMR for the halo region overhanging the solar neighborhood. See Fig. 1 caption for key to abbreviations.

by the IMF and is the same at all radii) is provided in a relatively oxygen-poor medium.

8. Figure 4 shows the AMR for the halo in the region above the solar neighborhood. Comparing this with Schuster & Nissen's (1991) data, we can see that they are very well reproduced. This result and the ratio between the present masses in the halo and in the disk (~ 4–5×10^{-2}) confirm that the multiphase approach is a correct way to describe the interactive evolution of halo and disk.

9. We evaluated the present day mass function (PDMF) starting from the IMF and the model's result about SF history (see Paper II for details). The PDMF for the solar ring is plotted in Figure 5*a* compared with the observed functions reported by Scalo (1986) and Rana (1991). All the curves are normalized to the total mass under the distribution. Since our theoretical IMF had its parameters adjusted to provide reasonable agreement with the observed IMF as derived from the PDMF and since our SFR histories are rather smooth, the theoretical IMF naturally yields a PDMF that agrees with observations. We are then allowed to propose predictions for not yet observed PDMFs; in particular, for the outer and inner rings, we evaluate the corresponding distributions, plotted in Figure 5*b*. For convenience, we maintain an IMF constant in time and space, considering it is unnecessary to elaborate on this and lacking firm evidence on how to proceed otherwise.

Although derived very simply from the previous one for the solar neighborhood, which presented the difficulties discussed in Paper II, leading to the introduction of a thick disk component, this first model already gives surprisingly good results: gas fraction distribution, oxygen gradient, and radial variation of the SFR are reasonably well understood. To analyze the effect of the assumptions about the infall rate on disk evolution, in models B and C we changed the length scale, l, that is, the radial decay of the infall parameter f, with respect to the value assumed for the solar ring. While in model A we had $l = 2$ kpc, we assume $l = 4$ kpc in model B and $l = 1$ kpc in model C. In Figure 6 the radial distributions of gas fraction (Fig. 6*a*), oxygen abundance (Fig. 6*b*), and star formation rate (Fig. 6*c*) are shown for $t = 13$ Gyr for models A, B, and C. In model C the infall timescale at $R = 4$ kpc takes a value 0.018 Gyr less than in model A (0.14 Gyr), while at $R = 12$ kpc the infall timescale for models C and A take the values 55 Gyr and 7.5 Gyr, respectively. As expected from the above discussion, this more concentrated infall produces a rather steep distribution of gas and a high degree of depletion in the SFR radial distribution, which do not correspond to observations. However, despite the obvious flattening in the internal rings where the evolution is almost completed, the metallicity gradient has the observed slope at solar radius, due to an increased difference of evolutionary level between external and internal rings.

In contrast, model B with its slower infall decrease should be preferred on the basis of SFR and gas fraction distributions and ruled out because of its flatter oxygen abundance. Anywhere, almost all the constraints could be fit by this model. We recall that, e.g., Götz & Köppen (1992) and Lacey & Fall (1985), selected as the best value $l = 3.5$ kpc.

We also run models varying the timescale of collapse for $R = 8$ kpc, maintaining the scale length of accumulation $l = 2$ kpc: τ_{coll} takes the value 0.5 Gyr in model D and 2 Gyr in model E. In Figure 7 the same relations as in Figures 1 and 2 are presented, for models A, D, and E, at present time.

The effects of the infall timescale on SFR and linked relations discussed above help us to understand the different evo-

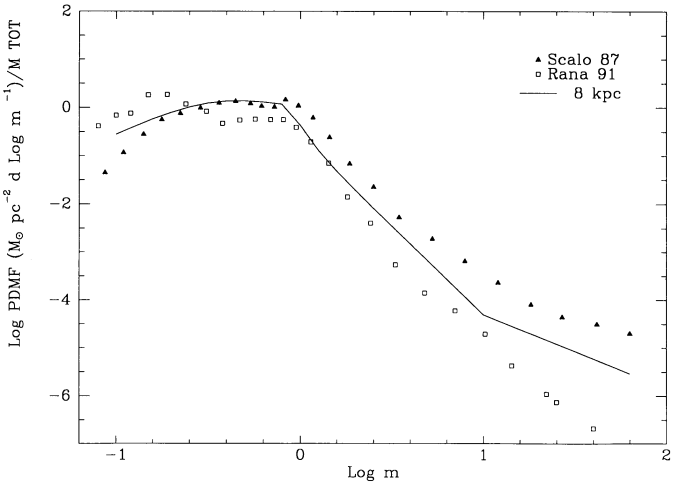

FIG. 5*a*

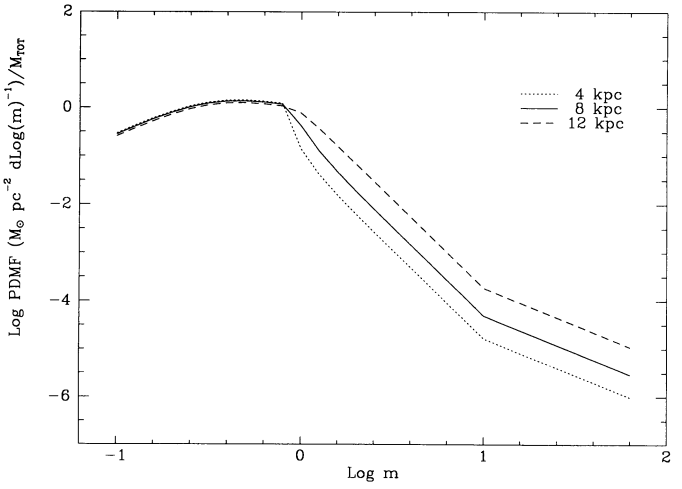

FIG. 5*b*

FIG. 5.—PDMF evaluated from model A (*a*) in the solar neighborhood, superimposed on data from Scalo (1987; *triangles*) and Rana (1991; *squares*), and (*b*) for inner, solar, and outer regions.

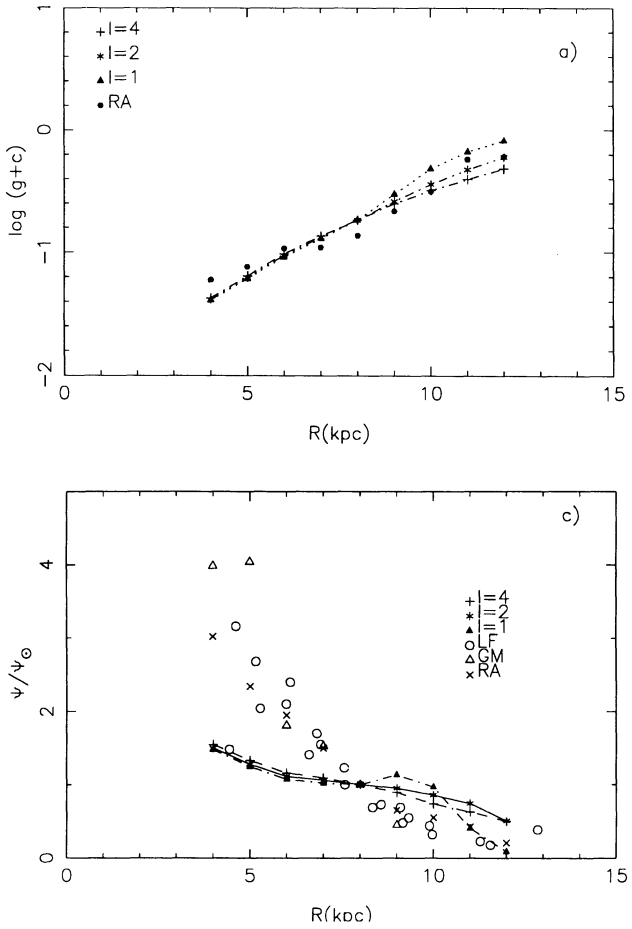

FIG. 6.—Models A, B, and C with $l = 2$, 4, and 1 kpc, respectively. Radial variations of (*a*) gas fraction, (*b*) oxygen abundance, and (*c*) SFR, at $t = 13$ Gyr.

lutionary histories. In fact, the highest infall rate (model D, which has the shortest collapse times) produces, as might be expected, a much higher SFR at early times ($\psi_{\max,D} \sim 22$ vs. $\psi_{\max,E} \sim 7$): the system soon has at its disposal a large quantity of gas that can be converted into stars at a high rate. As a consequence, the metal enrichment as a function of time (AMR) is steeper and reaches the asymptotic value sooner. The oxygen gradient is flatter, because evolution is more rapid and efficient at all radii, favoring an almost complete saturation of the enrichment, and the gas fraction distribution is lower than observed.

In contrast, the slowest timescale (model E) will produce a lower SFR at every radius. From Figure 7, it can be seen that model E provides as good a fit as model A for all the observational relations, except for the AMR, whose flattening is not achieved in the necessary time.

In her analysis, Tosi (1988) concluded that if one assumes an exponentially decreasing infall, its *e*-folding time must have been larger than the Galactic age, and Götz & Köppen (1992) fix $\tau_f = 15$ Gyr, so that disk formation and evolution look like very slow processes. On the basis of such enrichment timescales and halo-disk mass ratio, in Paper II we chose $\tau_{\rm coll} \sim 2$ Gyr as the best infall timescale in the solar zone.

Finally, we tested the influence of changing the total mass of the Galaxy, assigning ring masses with different prescriptions for the absolute value of the present surface mass density in the disk as well as for the radial decrease law. This test provides both an estimate of the effects of errors on the assumed galactic mass and predictions about radial properties of galaxies of different masses. We ran three models with different assumptions about ring masses as listed in Table 5 and with the same coefficients as in model A. As expected, the SFR is more efficient by a factor of 2 for the most massive disk and the gas density is lower; the O gradient is steeper for the lowest disk, which evolves at a slower speed than the others (see Fig. 8).

5. SUMMARY AND CONCLUSIONS

The simultaneous fulfillment of observational constraints limits the possible galactic evolutions; a few conclusions can be drawn from our analysis:

1. Gradients for element abundances and gas density can be obtained by varying the SFR among zones at different galactocentric radii, as a consequence of higher gas density, cloud formation efficiency, and high gas replenishment rate in central regions. The amount of this variation for each galaxy is constrained by the steepness of element gradients and by the galactic age.

2. If a present of 13 Gyr is accepted for the disk, only $\tau_{\rm coll} \simeq$ 1–2 Gyr is acceptable for the gas, element abundance, and SFR gradients; the corresponding AMR and SFR versus time are in close agreement with observations. Younger ages for the disk could correspond to slower collapses.

3. If $f(r)$ has a short length scale, gradients are present only if SF is a slow process. The difference between the mass scale

TABLE 5

TOTAL RADIAL MASS DISTRIBUTION

R (kpc)	MODEL 1	2	3
4.0	6.0[a]	9.0	3.00
5.0	5.0	7.5	2.50
6.0	4.0	6.3	2.00
7.0	3.5	5.3	1.70
8.0	3.0	4.5	1.50
9.0	2.5	3.8	1.20
10.0	2.0	3.0	1.00
11.0	1.7	2.5	0.85
12.0	1.4	2.1	0.70

[a] Units are $10^9\ M_\odot$.

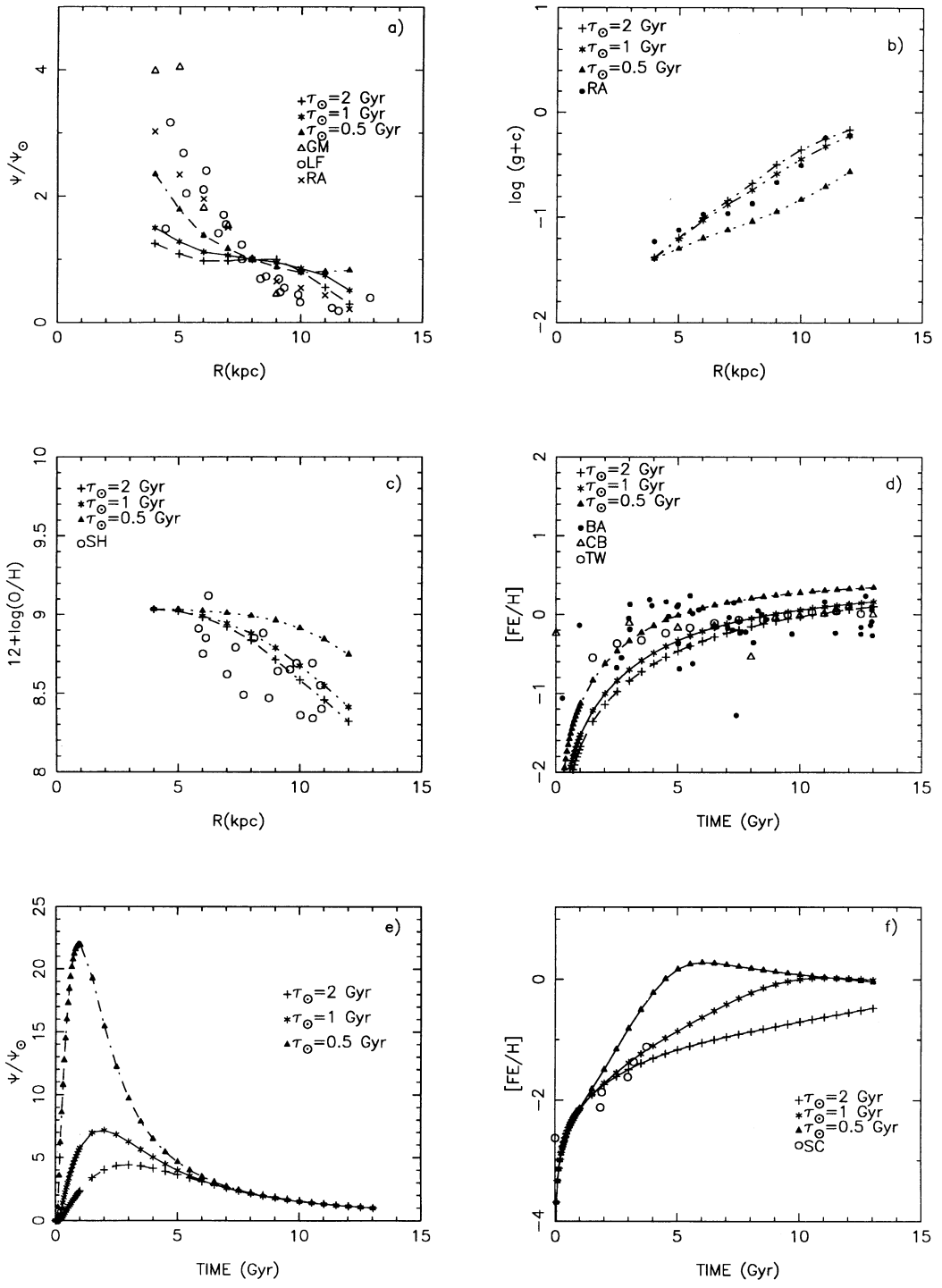

FIG. 7.—Models A, D, and E with τ_{coll} = 1, 0.5, and 2 Gyr, respectively. (*a*) SFR "today," (*b*) total gas fraction, (*c*) oxygen gradient, (*d*) AMR in the solar neighborhood, (*e*) SFR for the solar neighborhood, and (*f*) AMR for halo. See Fig. 1 caption for key to abbreviations.

length and the infall scale length determines the present radial distribution of the SFR. The reproduction of the observed SFR distribution, as well as the gas density distribution, requires that the two lengths be comparable. In contrast, the abundance gradients are too flat for 13 Gyr, and from this last point of view it would be more appropriate to adopt $l = 1$ kpc.

4. Abundance gradients invariably flatten with time: the galactic system evolves toward saturation; the slopes can be different according to the evolutionary stage of the ring (lower in the center than at the periphery).

5. The SFR in the central regions decreases appreciably with time: internal regions in spiral galaxies appeared much bluer in the past.

6. The SFR does not depend on the total gas in a simple way in order to reproduce both atomic and molecular radial gas distributions.

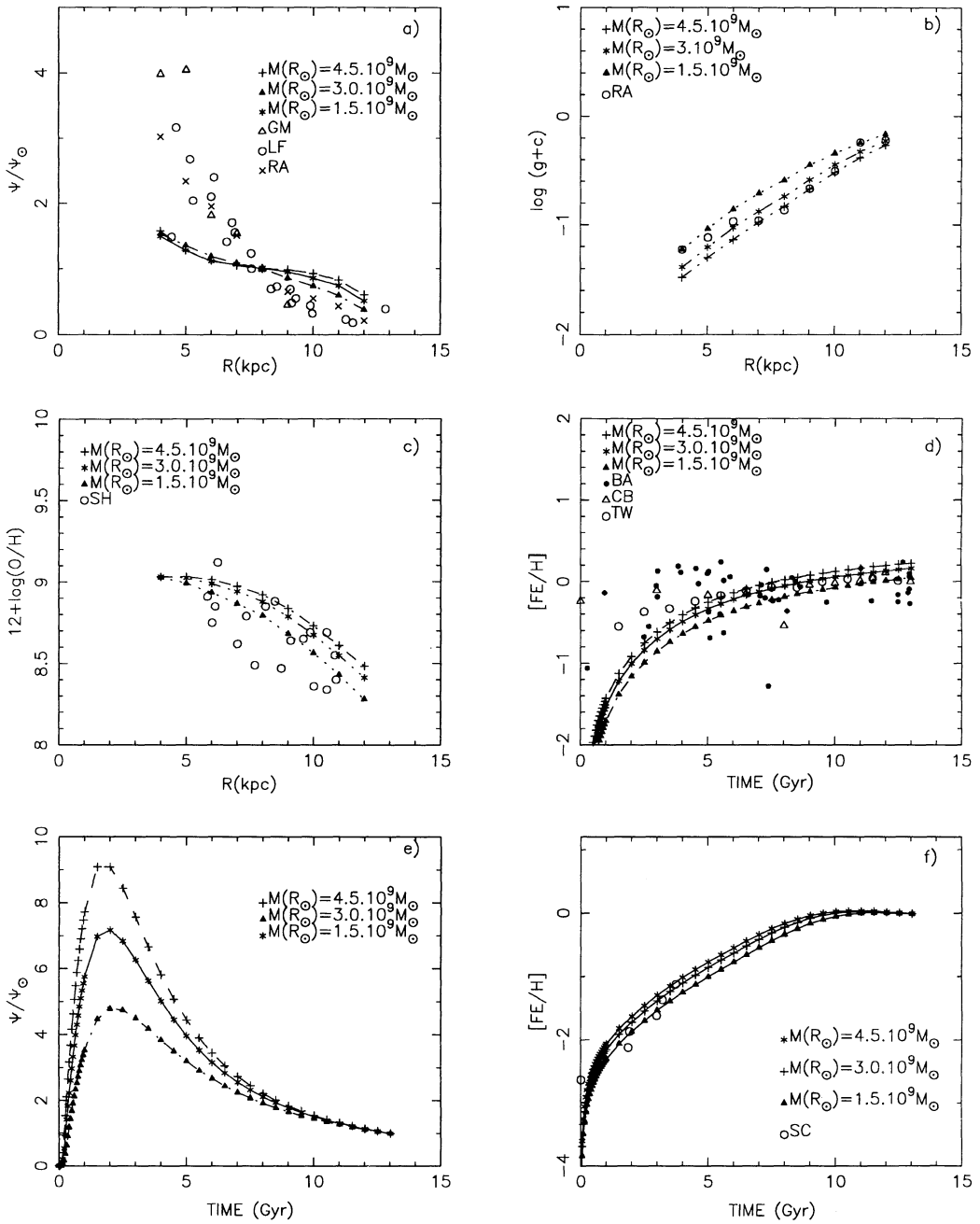

FIG. 8.—As Fig. 7, for models A, F, G and $M(R_\odot) = 3$, 4.5, and $1.5 \times 10^9\ M_\odot$, respectively. See Fig. 1 caption for key to abbreviations.

7. The AMR for both the solar region and outer regions are well reproduced; in particular, the lower slope for the external region is evident in most models, the consequence of slower SF activity and a different accretion from low-metal material coming from the halo.

8. More massive galaxies (galaxies with higher volumetric mass density) have higher SFR in the past and then enrich more efficiently, producing present flatter gradients.

As a final comment, we stress that qualitative behaviors, i.e., scaled to absolute values, are rather well reproduced. Indeed, they depend on the intrinsic nature of the model: self-regulation, the proper treatment of SF, and a multiphase structure.

The absolute values are instead fixed based on how many and which zones are considered: we have already stressed the necessity of introducing the thick disk phase, in Paper II; we will now add the bulge component. A fine tuning of SF in different zones will probably give the right solution for understanding the global structure of the Milky Way.

We want to thank U. Penco for discussions on the computational aspects of the present work. F.F. acknowledges support from MURST 40%. M.M. would like thank the Sezione di Astronomia, Università di Pisa, where this paper was partially written, for its hospitality.

REFERENCES

Arnett, D. W. 1991, in Frontiers of Stellar Evolution, ed. D. A. Lambert (ASP Conf. Ser., 20), 389 (A)
Barry, D. C. 1988, ApJ, 334, 436
Branch, D., & Nomoto, K. 1986, A&A, 164, 113
Burkert, A., & Hensler, G. 1988, A&A, 199, 131
Carlberg, R. G., Dawson, P. C., Hsu, T., & VanderBerg, D. A. 1985, ApJ, 294, 674
Cameron, L. M. 1985, A&A, 147, 47
Castellani, V., Chieffi, A., & Straniero, O. 1990, ApJS, 74, 463
———. 1992, ApJS, 78, 517
Clarke, C. J. 1989, MNRAS, 238, 283
Clifford, P., & Elmegreen, B. G. 1983, MNRAS, 202, 629
Díaz, A. I. 1989, in Evolutionary Phenomena in Galaxies, ed. J. E. Beckman & B. E. J. Pagel (Cambridge: Cambridge Univ. Press), 356
Díaz, A. I., & Tosi, M. 1984, MNRAS, 208, 365
———. 1986, A&A, 159, 49
Faúndez-Abans, M., & Maciel, W. J. 1986, A&A, 158, 228
Ferrini, F. 1991a, in Chemical and Dynamical Evolution of Galaxies, ed. F. Ferrini, F. Matteucci, & J. Franco (Pisa: Editrice Tecnico Scientifica), 511
———. 1991b, in Evolution of Interstellar Matter and Dynamics of Galaxies, ed. J. Palouš, W. B. Burton, & P. O. Lindblad (Cambridge: Cambridge Univ. Press), 304
———. 1993, in Star Formation, Galaxies and the Interstellar Medium, ed. J. Franco, F. Ferrini, & G. Tenorio-Tagle (Cambridge: Cambridge Univ. Press), 378
Ferrini, F., & Galli, D. 1988, A&A, 195, 27
Ferrini, F., Marchesoni, F., & Vulpiani, A. 1983, MNRAS, 202, 1071
Ferrini, F., Matteucci, F., Pardi, C., & Penco, U. 1992, ApJ, 387, 138 (Paper I)
Ferrini, F., Palla, F., & Penco, U. 1990, A&A, 213, 3
Fich, M., & Silkey, M. 1991, ApJ, 366, 107
Fitzsimmons, A., Dufton, P. L., & Rolleston, W. R. J. 1992, MNRAS, 259, 489
Franco, J. 1991, in Chemical and Dynamical Evolution of Galaxies, ed. F. Ferrini, F. Matteucci, & J. Franco (Pisa: ETS), 506
———. 1992, in Star Formation in Stellar Systems, ed. G. Tenorio-Tagle, M. Prieto, & F. Sanchez (Cambridge: Cambridge Univ. Press), 515
Geisler, P. 1987, AJ, 94, 84
Gilmore, G., Wyse R. F. G., & Kuijken, K. 1989, ARA&A, 27, 555
Götz, M., & Köppen, J. 1992, A&A, 262, 455
Güsten, R., & Mezger, P. G. 1983, Vistas Astron., 26, 159
Harris, H. C. 1981a, AJ, 86, 707
———. 1981b, AJ, 86, 719
Hashimoto, M., Iwamoto, K., & Nomoto, K. 1993, ApJ, 414, L105
Hausman, M. A., & Roberts, W. W. 1984, ApJ, 282, 106
Kennicutt, R. C. 1989, ApJ, 344, 685
Lacey, C. G., & Fall, S. M. 1983, MNRAS, 204, 791
———. 1985, ApJ, 290, 154
Lewis, J. R., & Freeman, K. C. 1989, AJ, 97, 139
Maeder, A. 1983, A&A, 120, 113
———. 1992, A&A, 264, 105 (M)
Matteucci, F., François, P. 1989, MNRAS, 239, 885
Mead, K., Kutner, M. L., & Evans, N. 1990, ApJ, 354, 492
Meyer, J. P. 1988, in Cosmic Abundances of Matter, ed. C. J. Waddington (AIP Conf. Proc. 183), 245
Mollá, M., Díaz, A. I., & Tosi, M. 1991, in Chemical and Dynamical Evolution of Galaxies, ed. F. Ferrini, F, Matteucci, & J. Franco (Pisa: ETS), 577
Mollá, M., Ferrini, F., Díaz, A. I., & Pardi, C. 1992, in Proc. 3d DAEC Meeting on the Feedback of Chemical Evolution on the Stellar Content of Galaxies, ed. D. Alloin & G. Stasinska (Paris: Imprimerie de Paris), 258
Nissen, P. E., & Edvardsson, B. 1992, A&A, 261, 255
Nomoto, K., & Kondo, K. 1991, ApJ, 367, L19
Nomoto, K., Thielemann, F. K., & Yokoi, K. 1984, ApJ, 286, 644
Oey, M. S., & Kennicutt, R. C. 1993, ApJ, 411, 137
Pagel, B. E. J. 1989, in Evolutionary Phenomena in Galaxies, ed. J. E. Beckman & B. E. J. Pagel (Cambridge: Cambridge Univ. Press), 201
Panagia, N., & Tosi, M. 1981, A&A, 96, 306
Pardi, M. C., & Ferrini, F. 1994, ApJ, 421, 491
Parravano, A. 1989, ApJ, 347, 812
Peimbert, M., & Serrano, A. 1982, MNRAS, 198, 563
Phillips, S., & Edmunds, M. G. 1991, MNRAS, 251, 84
Rana, N. C. 1991, ARA&A, 29, 129
Renzini, A., & Voli, M. 1981, A&A, 94, 175
Sanders, D. B., Solomon, P. M., & Scoville, N. Z. 1984, ApJ, 276, 182
Sandrelli, S. 1994, Mem. Soc. Astron. Ital., in press
Scalo, J. M. 1986, Fund. Cosm. Phys., 11, 1
Schaerer, D., Meynet, G., Maeder, A., & Schaller, G. 1993, A&ASS, 98, 523
Schaller, G., Schaerer, D., Meynet, G., & Maeder, A. 1992, A&ASS, 96, 269
Schattenburg, M. L., & Canizares, C. R. 1986, ApJ, 301, 759
Schuster, W. J., & Nissen, P. E. 1989, A&A, 222, 69
Shaver, P. A., McGee, R. X., Newton, L. M., Banks, A. C., & Pottash, S. R. 1983, MNRAS, 204, 53
Sodroski, T. J. 1991, ApJ, 366, 95
Sommer-Larsen, J., & Yoshii, Y. 1989, MNRAS, 238, 133
Talbot, R. J., & Arnett, D. W. 1973, ApJ, 186, 51
Timmes, F. X., Woosley, S. E., & Weaver, T. A. 1993, in Proc. 6th Advanced School of Astrophysics in São Paolo, ed. B. Barbuy, J. A. de Freitas Pacheco, & E. Janot-Pacheo (São Paolo: Instituto de Geociencias e Astronomia, Univ. São Paolo)
Tinsley, B. M. 1980, Fund. Cosm. Phys., 5, 287
Tosi, M. 1988, A&A, 197, 33
Tosi, M., & Díaz, A. I. 1985, MNRAS, 217, 571
Tsujimoto, T., Iwamoto, K., Hashimoto, M., Momoto, K., & Thielemann, F.-K. 1993, in The Origin and Evolution of the Elements, ed. S. Kubono & T. Kajino (Singapore: World Scientific), 217
Twarog, B. A. 1980, ApJ, 242, 242
Woosley, S. E., Pinto, P. A., & Weaver, T. A. 1988, Proc. Astron. Soc. Australia, 355
Woosley, S. E., & Weaver, T. A. 1986, in IAU Colloq. 89, Radiation Hydrodynamics in Stars and Compact Objects, ed. D. Mihalas & K. A. Winkler (Berlin: Springer), 91 (WW)
Wyse, R. F. G., & Silk, J. 1989, ApJ, 339, 700
Zinn, R. 1985, ApJ, 293, 424